International Journal of Environmental Sciences
ISSN: 2229-7359
Vol. 10 No. 4, 2024
https://theaspd.com/index.php/ijes/index

Green Synthesis And Spectral Characterization Of Molybdenum Trioxide Nanoparticles From Costus Pictus Leaves Extract

V. Vithya[1,2], K. Sathiyamoorthi[1], S. Darlin Quine[1*]
[1]PG & Research Department of Chemistry, Government Arts College, B-Mutlur, Chidambaram-608102.
[2]Department of Chemistry, Dharmapuram Gnanambigai Government Arts College for Women, Mayiladuthurai-609001
Corresponding Author: S. Darlin Quine, darlinmainzen728@gmail.com

Abstract
This study aims to green synthesize of Molybdenum (MoO_3) nanoparticles mediated by Costus pictus (Insulin plant) leaves. This is a rare medicinal species of flowering shrub with religious significance. The green synthesized Molybdenum trioxide nanoparticles are calcinated at 350° C, then characterized by Ultra violet spectroscopy, Infrared spectroscopy, XRD and SEM with EDS analysis, UV Spectroscopy produced optical property of this nanoparticles, FTIR have showed to evident peaks were appeared in the molybdenum iron peaks, XRD have explain crystalline and nature of bimetallic nanoparticles, SEM shows the various micrographic images of Molybdenum trioxide nanoparticles, EDS have shown the chemical purity of Molybdenum trioxide nanoparticles. The Green chemistry, also called sustainable chemistry, is an area of chemistry and chemical engineering focused on the design of products and processes that minimize or eliminate the use and generation of hazardous substances.

Keywords: *Green synthesis, Costus pictus, MoO3, UV, FT-IR, XRD, SEM and EDS*

1. INTRODUCTION

Nanotechnology has emerged as a powerful tool in many fields of science and engineering due to its focus on altering and enhancing materials on a nanoscale scale [1]. It is a fascinating domain to alter the materials in size, shape, morphology and dimensions, creating nanoparticles almost equal to the Bohr radius [2]. Green technology, which includes the employment of microorganisms like bacteria, fungi, yeast and plant material extract as a safe and eco-friendly tool for synthesizing nanoparticles, has taken the lead over physical and chemical methods [3, 4]. Therefore, biogenic preparation of metal nanoparticles is extremely popular nowadays. Owing of existence of phytochemicals like flavonoids, terpenoids and quinines phenols, alkaloids and tannins plant-mediated synthesis has become a powerful unconventional instrument for synthesizing nanoparticles [5, 6]. The phytonutrients are playing significant role in governing particle size *via* prompting and topographical reactions and performing role of capping agents [7]. Molybdenum has gained much attention owing to its wide range applications [8, 9]. Since molybdenum exist in various oxidation states and having low toxicity than other *d*-block elements thus, molybdenum nanoparticles are made to absorb, to cure many deficiency disorders. The deficiency may sometimes disrupt enzyme activity in nitrogen metabolism [10, 11]. Molybdenum oxide derivatives due to their distinctive electrochemical and diverse topography are one of the captivating transition metal oxides [12]. Molybdenum oxide a verified chemical for various uses, primarily for Li-ion battery [13]. Still, a few reports have also used them to decontaminate water [14]. Even though several reports are available which are explaining the amazing photocatalytic activity of molybdenum trioxide (MoO3) [15], though, few studies are there to examine the photocatalytic activity of MoO2 [16]. Surface active ingredients are important tools to carve the morphological structure of nanoparticles, which in turn alters the property of material [17]. A little research support is there to describe the geomorphological controlled preparation of molybdenum oxide [18]. Of late, MoO3 nanostructures display photocatalytic properties under UV-visible light. With the nanoparticles of MoO3 under visible light, several applications have been explored and examined, such as photosensitive deterioration of methylene violet dye [19,20] and methylene orange dye [21], gas sensing properties [22], supercapacitor [23], oxidation of methanol [24], epoxidation [25], light/optical properties [26], lithium storing capabilities [27]. The reduction property of

MoO3 in presence of light interconnects with the particles' chemical properties, shape and size. Several synthetic approaches have revealed two different phases (h- and α-phases) of MoO3 [28]. Nanorod's morphologies were explained and exhibited the hphase though another phase (a) resembles nanowires and plates [29,30]. In literature, many traditional electrode materials have been applied to eradicate harmful pollutants for sensor applications of Fe2O3, Co2O3, CuO, TiO2 and molybdenum oxide, which are a few significant examples [31]. This research work summarizes our investigation in green synthesis, characterization of molybdenum oxide nanoparticles, the synthesized nanoparticles characterized by ultraviolet-visible spectroscopy, FTIR spectroscopy, X-ray diffraction, SEM and EDS analysis have shown excellent outcome,

2. MATERIAL AND METHODS

2.1. Collection of Sample

Fresh and healthy leaves of *Costus pictus* were collected from private botanical vandigate, Chidambaram. Leaves were washed in three times thoroughly by running ordinary tap water (OTW), and then washed two times with double distilled water (DDW) to remove any dust particles on the leaves. Washed leaves were allowed to dry in air at room temperature. The dried leaves were grained and powdered by using electric mixer. This powder was used to prepare the leaves extracts

2.4. Plant material processing

5 grams of healthy *Costus pictus* healthy leaves powder with 50 mL of double-distilled water (DDW) taken in the 250 mL round bottomed flask, water condenser fitted and fix the running tap water then heated for 20 min at 80O C. Then the extract was filtered with Whatman 1≠ filter paper. The filtrate was used for further green synthesis of process

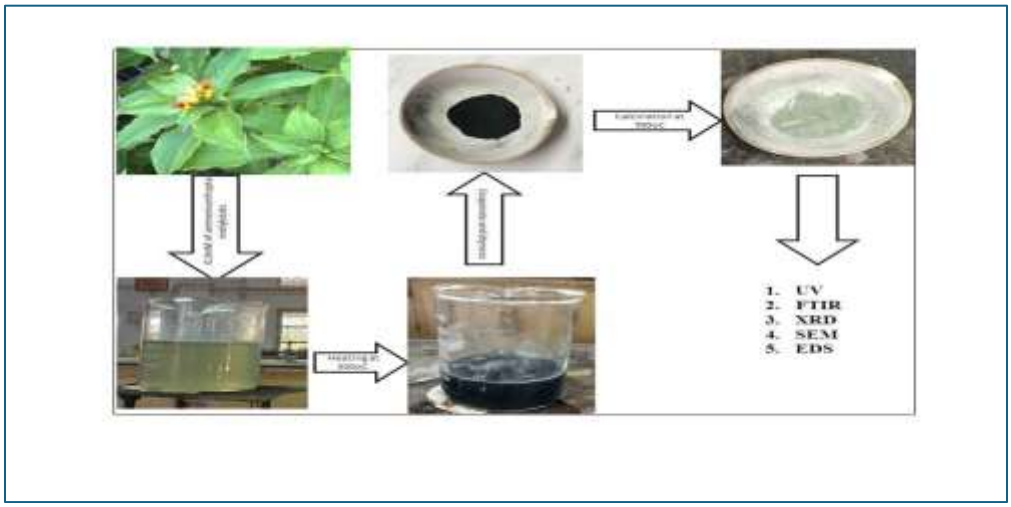

Figure:1 Green synthesis of Molybdenum oxide nanoparticles by *Costus pictus* (Insulin plant) leaves extract

2.5. Biosynthesis procedure

For the synthesis of molybdenum trioxide nanoparticles by reducing ammonium molybdate hexahydrate, 180 mL of homogenous solution of ammonium molybdate hexahydrate is steadily mixed with 10mL of leaves extract followed by continuous heating (70 °C) and stirring at 500 rpm for 3 hr at magnetic stirrer with heating instrument, to achieve brownish solution [32]. The precipitate was dried and powdered then calcinated at 350oC through muffle furnace. After calcination to obtained milky white colour fine crystalline molybdenum oxide nanoparticles. Finally, Mo2O3NPs were steadily characterized. Figure.1, have shown in scheme of green synthesis of molybdenum oxide nanoparticles.

2.4 Characterizations of Mo_2O_3 Nanoparticles

3. RESULT AND DISCUSSION

International Journal of Environmental Sciences
ISSN: 2229-7359
Vol. 10 No. 4, 2024
https://theaspd.com/index.php/ijes/index

3.1 UV Spectral Analysis

UV–vis absorption spectra were recorded for MoO3NPs in the range of 200–1200 nm using an aqueous MoO3NPs suspension. The samples displayed an optical absorption peaks of absorption maximum value have been shown 224.25 nm for all the nanoparticle suspension but concentrations increases absorption (a,u) only increases. The increasing shift of the UV–vis peak of Mo3O4NPs may be due to the aggregation of the nanoparticles as a molybdenum oxide nano-assemblage. The dynamic absorption peaks are shown at 323 nm is evidence of the existence of various organic compounds that interact with molybdenum oxide ions in solution and implies a possible course for the reduction of the metal ions present in the solution the merged UV spectrum had been shown in **Figure:2**.

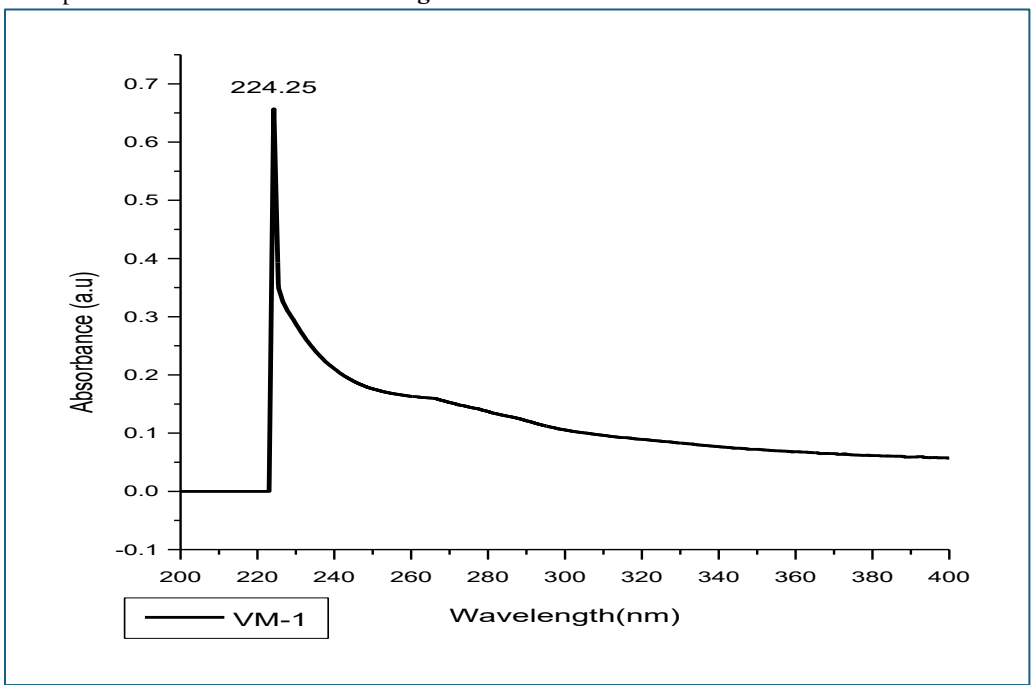

Figure:2 UV Spectrum of Molybdenum oxide nanoparticles by *Costus pictus* (Insulin plant) leaves extract

3.2 FT-IR Spectroscopy

The FTIR analysis was further performed to determine the phyto-constituent containing functional groups involved in synthesizing Mo3O4NPs as reducing and capping agents. **Figure:3** presented the FTIR spectrum of plant leaf extract and nanoparticles. The results of Mo3O4NPs FTIR spectrum demonstrated that the frequency of 3439 cm-1 at the very broad peak represent the various stretching frequencies are merged to appeared it, this peak had been screened out -O-H group in alcohols and acids, the very sharp peak at 2026 cm-1 have shown in Carbon carbon triple bond intensity, The sharp stretching frequency of 1583 cm-1 have represented by -C=O- group contain functional groups of aldehyde, acid and its derivatives. -N-H group in amide, -C=N nitrile, -C-H aromatic stretching and aldehydic –CH stretching frequencies, frequency of 1404 cm-1 is represent in N-H bending) , strong peak of 1022 cm-1-C-H bending in gem dimethyl, -OH bending vibration have shown in the frequency 675 cm-1have shown in Mo-O stretching vibrations[31] . These results suggest that many biologically active phyto-molecules are left adsorbed on the surface of the MoO3NPs

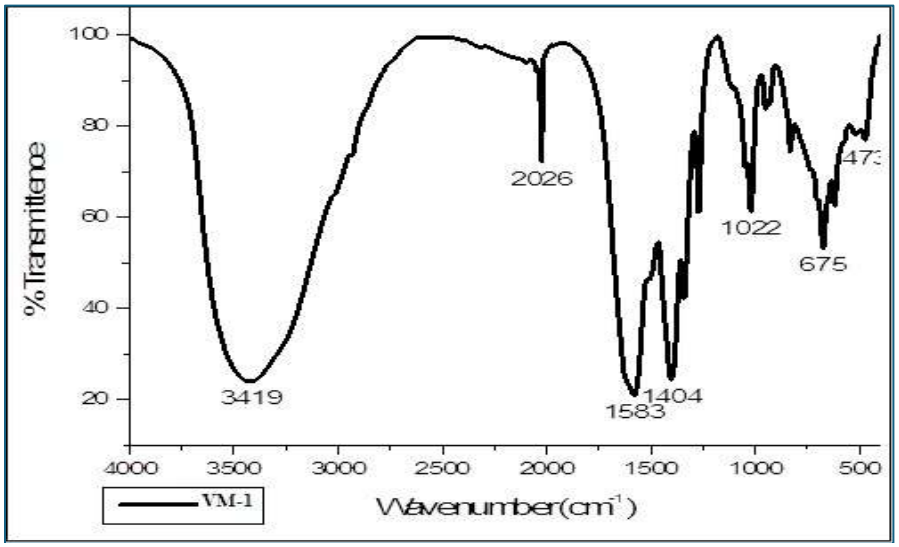

Figure:3 FT-IR Spectrum of Molybdenum oxide nanoparticles by *Costus pictus* (Insulin plant) leaves extract

3.3 XRD Analysis

The XRD analysis was done to confirm that the obtained product was molybdenum trioxide. The XRD was done by Cu K-alpha radiation (1.54 Ao). The structure of MoO3 nanoparticles synthesized had an orthorhombic phase.

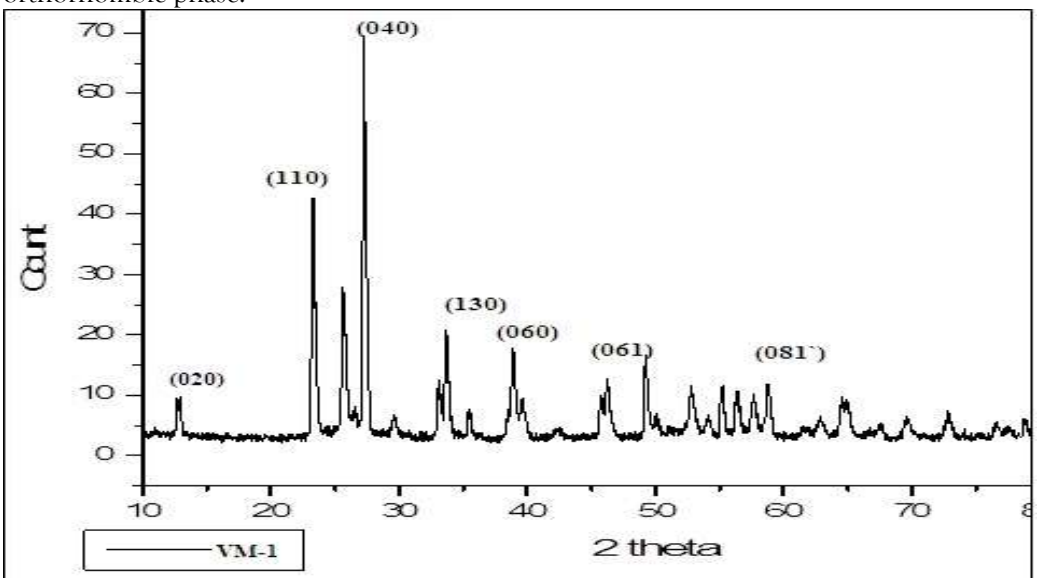

Figure:3 XRD pattern of Molybdenum oxide nanoparticles by *Costus pictus* (Insulin plant) leaves extract

The XRD peaks were observed at 12.8°(020), 23.5° (110), 27.3° (040), 33.6° (130), 39.1° (060), 49.3° (061) and 58.9° (081). The product was confirmed to be MoO_3 by comparing the peak values with JCPDS software, the peak values matched with JCPDS card No.29-0115

1/d2 =(h2+k2+l2)/a2..... **(1)**

The unit cell volume (V) was calculated as third power of the lattice constant and found as 158.813 Å3. Debye-Scherrer formula (equation 4) was used to determine the average crystallite size of the particles:

D =0:9λ/βcosθ .....**(2)**

Where D is the average crystallite size, λis the wavelength of X-ray used (1.54060 Å), β is the angular peak width at half maximum (rad) and θ is Bragg's diffraction angle. The average crystallite size was estimated as 41.42 nm for MoO_3.

3.4 SEM and EDS

The morphology determined by SEM analysis of green synthesized MoO_3 nanoparticle by *Costus pictus* (Insulin plant) leave extract has shown, **Figure:4.** It can be seen from SEM image that MoO_3NPs are agglomerated and not well formed[32]. One can vividly see well defined nanoparticles with distinguish shapes. Specifically, SEM image for MoO_3NPs reveal distinguishable rhomboid shaped nanoparticles, elongated nanorods and highly agglomerated nanoparticles. MoO_3 nanoparticles become well-formed reveling distinct shapes. To identify chemical elements and purity of synthesized samples **Figure:5** have shown in 1-20 μm.

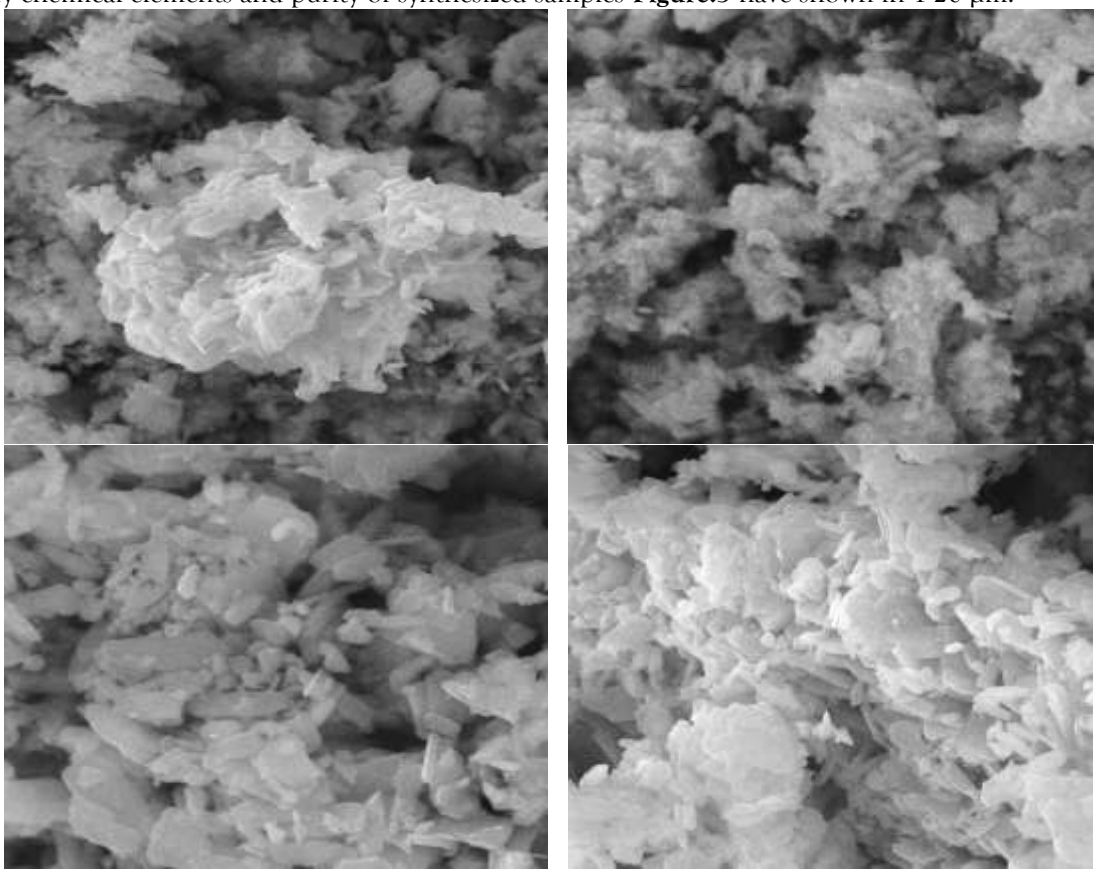

Figure:4 SEM micrography of Molybdenum oxide nanoparticles by *Costus pictus* (Insulin plant) leaves extract

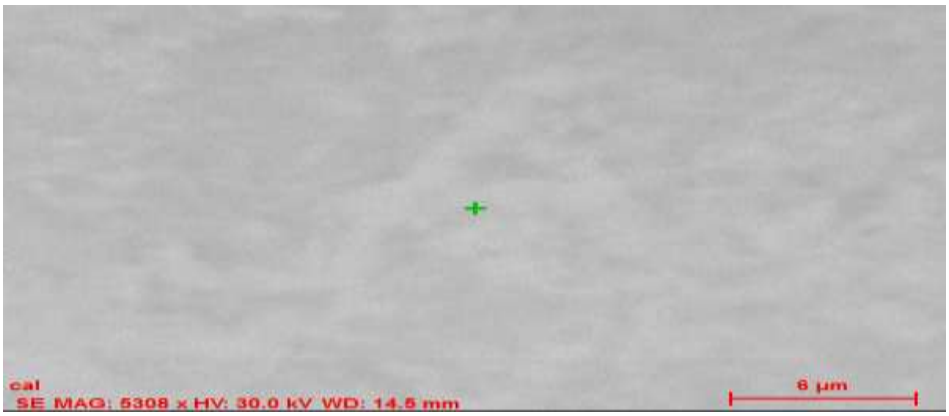

Figure:5 EDS micrography of Molybdenum oxide nanoparticles by *Costus pictus* (Insulin plant) leaves extract

International Journal of Environmental Sciences
ISSN: 2229-7359
Vol. 10 No. 4, 2024
https://theaspd.com/index.php/ijes/index

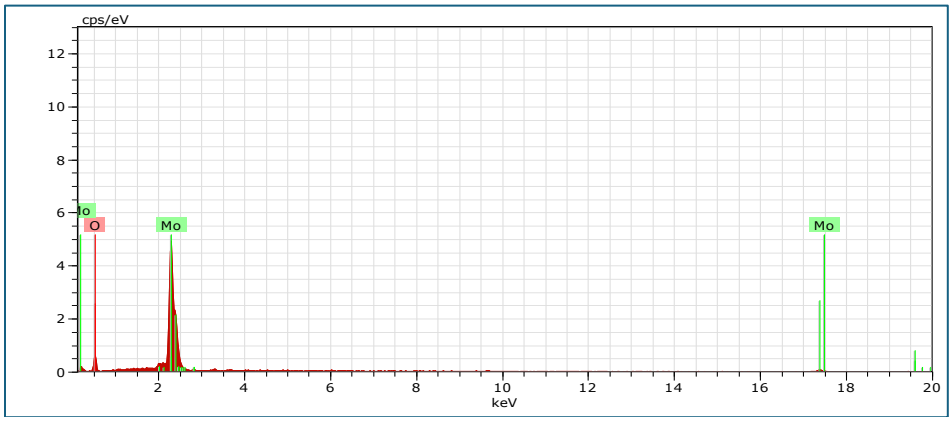

Figure:6 EDS spectrum of Molybdenum oxide nanoparticles by *Costus pictus* (Insulin plant) leaves extract

EDS analysis were performed and results are shown in **Figure.6** According to EDS spectra, the most pronounced and only chemical elements presents on samples are O and Mo. Cleary, there are no other chemical elements identified in the sample which confirm purity of synthesized sample as MoO3 nanoparticles. The sizes of the nanoparticle have shown in EDS image is 6 µm, gives the atomic percentages of chemical elements on samples. As one can see in this table, there are differences in the atomic percentages of the chemical elements in the different shape of nanoparticles

Table:3 Element percentage of EDS Results

S.No	Element	AN	%
1	O	8	83.89
2	Mo	42	16.11

4. CONCLUSION

The green synthesis of leaf extract of *Costus pictus* (Insulin plant) proved to be an effective reducing and stabilizing agent for the green synthesis of highly crystalline and extremely small sized MoO3. The reduction of the metal charged ions led to the pattern of metal nanoparticles of fairly well-defined dimensions using the extract. The UV-Vis, and FT-IR studies revealed the formation of MoO3. XRD analysis validated the presence of highly monodisperse nanoparticles of molybdenum trioxide. SEM images confirmed that the MoO3 NPs possessed octahedral morphology with the average size of 42.35 nm. This green chemistry approach towards the synthesis of MoO3 NPs has many advantages such as environmental friendly, cost effective and easily scaled up to large scale synthesis.

REFERENCE

1. S.H. Baker, M. Lees, M. Roy and C. Binns, *J. Phys. Condens. Matter*, **25**, 386004 (2013); https://doi.org/10.1088/0953-8984/25/38/386004
2. H.P.T. Nguyen, S. Arafin, J. Piao and T.V. Cuong, *J. Nanomater.*, **2016**, 2051908 (2016); https://doi.org/10.1155/2016/2051908
3. A.K. Mittal, Y. Chisti and U.C. Banerjee, *Biotechnol. Adv.*, **31**, 346 (2013); https://doi.org/10.1016/j.biotechadv.2013.01.003
4. M. Owais, A. Chauhan, Tufail, Sherwani, M. Sajid, C.R. Suri and M. Owais, *Int. J. Nanomedicine*, **6**, 2305 (2011); https://doi.org/10.2147/IJN.S23195
5. R. Nair, S.H. Varghese, B.G. Nair, T. Maekawa, Y. Yoshida and D.S. Kumar, *Plant Sci.*, **179**, 154 (2010); https://doi.org/10.1016/j.plantsci.2010.04.012
6. K. Sreevani and V.V. Anierudhe, *J. Biomater. Tissue Eng.*, **12**, 1071 (2022); https://doi.org/10.1166/jbt.2022.3021
7. R. Javed, M. Zia, S. Naz, S.O. Aisida, N. Ain and Q. Ao, *J. Nanobiotechnology*, **18**, 172 (2020); https://doi.org/10.1186/s12951-020-00704-4
8. C.A. Ellefson, O. Marin-Flores, S. Ha and M.G. Norton, *J. Mater. Sci.*, **47**, 2057 (2012); https://doi.org/10.1007/s10853-011-5918-5

9. B.N. Kaiser, K.L. Gridley, J.N. Brady, T. Phillips and S.D. Tyerman, *Ann. Bot. Seman. Sch.*, **96**, 745 (2005); https://doi.org/10.1093/aob/mci226
10. G.P. Awasthi, S.P. Adhikari, S. Ko, H.J. Kim, C.H. Park and C.S. Kim, *J. Alloys Compd.*, **682**, 208 (2016); https://doi.org/10.1016/j.jallcom.2016.04.267
11. A. Kumar and G. Pandey, *Am. J. Nanosci.*, **3**, 81 (2017).
12. Z. Wei, Z. Hai, M.K. Akbari, D.C. Qi, K.J. Xing, Q. Zhao, F. Verpoort, J. Hu, L. Hyde and S. Zhuiykov, *Sens. Actuators B Chem.*, **262**, 334 (2018); https://doi.org/10.1016/j.snb.2018.01.243
13. X. Zhang, X. Song, S. Gao, Y. Xu, X. Cheng, H. Zhao and L. Huo, *J. Mater. Chem. A Mater. Energy Sustain.*, **1**, 6858 (2013); https://doi.org/10.1039/c3ta10399d
14. H. Hu, J. Xu, C. Deng and X. Ge, *Mater. Res. Bull.*, **51**, 402 (2014); https://doi.org/10.1016/j.materresbull.2013.12.056
15. A. Chithambararaj, N.S. Sanjini, A.C. Bose and S. Velmathi, *Catal. Sci. Technol.*, **3**, 1405 (2013); https://doi.org/10.1039/c3cy20764a
16. H.-M. Hu, J.-C. Xu, X.-Q. Ge, M. Sun, H. Xuan and K.-H. Zhang, *Wuji Huaxue Xuebao*, **30**, 60 (2014); https://doi.org/10.11862/CJIC.2014.060
17. R.B. Pujari, V.C. Lokhande, V.S. Kumbhar, N.R. Chodankar and C.D. Lokhande, *J. Mater. Sci. Mater. Electron.*, **27**, 3312 (2016); https://doi.org/10.1007/s10854-015-4160-3\
18. X. Chen, Z. Zhang, X. Li, C. Shi and X. Li, *Chem. Phys. Lett.*, **418**, 105 (2006); https://doi.org/10.1016/j.cplett.2005.09.138
19. A. Bhaskar, M. Deepa and T.N. Rao, *ACS Appl. Mater. Interfaces*, **5**, 2555 (2013); https://doi.org/10.1021/am3031536
20. Y. Chen, X. Di, C. Ma, C. Zhu, P. Gao, J. Li, C. Sun and Q. Ouyang, *RSC Adv.*, **3**, 17659 (2013); https://doi.org/10.1039/c3ra42319k
21. W. Cho, J.H. Song, J.-H. Kim, G. Jeong, E.Y. Lee and Y.-J. Kim, *J. Appl. Electrochem.*, **42**, 909 (2012); https://doi.org/10.1007/s10800-012-0470-9
22. B. Guo, X. Fang, B. Li, Y. Shi, C. Ouyang, Y.-S. Hu, Z. Wang, G.D. Stucky and L. Chen, *Chem. Mater.*, **24**, 457 (2012); https://doi.org/10.1021/cm202459r
23. Y. Lei, J. Hu, H. Liu and J. Li, *Mater. Lett.*, **68**, 82 (2012); https://doi.org/10.1016/j.matlet.2011.10.043
24. S.H. Choi and Y.C. Kang, *ChemSusChem*, **7**, 523 (2014); https://doi.org/10.1002/cssc.201300838
25. J. He, H. Wang, C. Gu and S. Liu, *J. Alloys Compd.*, **604**, 239 (2014); https://doi.org/10.1016/j.jallcom.2014.03.134
26. Y. Liang, S. Yang, Z. Yi, X. Lei, J. Sun and Y. Zhou, *Mater. Sci. Eng. B*, **121**, 152 (2005); https://doi.org/10.1016/j.mseb.2005.03.027
27. Y. Liang, S. Yang, Z. Yi, J. Sun and Y. Zhou, *Mater. Chem. Phys.*, **93**, 395 (2005); https://doi.org/10.1016/j.matchemphys.2005.03.034
28. Y. Liang, Z. Yi, S. Yang, L. Zhou, J. Sun and Y. Zhou, *Solid State Ion.*, **177**, 501 (2006); https://doi.org/10.1016/j.ssi.2005.12.001
29. J. Liu, S. Tang, Y. Lu, G. Cai, S. Liang, W. Wang and X. Chen, *Energy Environ. Sci.*, **6**, 2691 (2013); https://doi.org/10.1039/c3ee41006d
30. S. Liu, H. Yin, H. Wang, J. He and H. Wang, *Ceram. Int.*, **40**, 3325 (2014); https://doi.org/10.1016/j.ceramint.2013.09.102
31. N.P. Shetti, S.D. Bukkitgar, K.R. Reddy, C.V. Reddy and T.M. Aminabhavi, *Colloids Surf. B Biointerfaces*, **178**, 385 (2019); https://doi.org/10.1016/j.colsurfb.2019.03.013
32. L. Fang, Y. Shu, A. Wang, T. Zhang ., J. Phys. Chem. C 2007, 111, 6, 2401–2408, https://doi.org/10.1021/jp065791r